JOURNAL OF GEOPHYSICAL RESEARCH, VOL. 114, B04402, doi:10.1029/2008JB005727, 2009

Effect of the satellite laser ranging network distribution on geocenter motion estimation

X. Collilieux,[1] Z. Altamimi,[1] J. Ray,[2] T. van Dam,[3] and X. Wu[4]

Received 28 March 2008; revised 5 February 2009; accepted 12 February 2009; published 7 April 2009.

[1] SLR network translations estimated between a quasi-instantaneous station position set, theoretically expressed with respect to the center of mass of the Earth (CM), and a secular reference frame are the signature of the motion of the CM with respect to the Earth crust. Geocenter motion is defined here to be the motion of the CM with respect to the geometric center of the solid Earth surface (CF). SLR translational variations cannot be rigorously interpreted as identical to geocenter motion due to the sparse and nonuniform distribution of the SLR network. Their difference is called the network effect, which should be dominated at subdecadal timescales by loading signals. We have computed translation time series of the SLR network using two independent geophysically based loading models. One is a displacement model estimated from surface fluid data (Green's function approach), called forward model, and the other is a displacement model estimated from GPS and ocean bottom pressure (OBP) data, called inverse model. The translation models have been subtracted from their respective geocenter motion models computed from degree-1 mass load coefficients in order to evaluate their network effect biases. Scatter due to the SLR network effect is at the level of 1.5 mm RMS. It could slightly shift the phase of the annual SLR geocenter motion estimate by less than 1 month and could affect *X* and *Z* annual geocenter motion amplitudes at the 1-mm level, which is about one third of the expected signal. Two distinct methods are suggested to account for network effect when comparing SLR translations to geocenter motion models. The first is to add the network effect term predicted by a displacement model to the geocenter motion loading model. The second relies on an adequate combination of SLR and GPS products to estimate SLR translation that could be better compared with geocenter motion.

Citation: Collilieux, X., Z. Altamimi, J. Ray, T. van Dam, and X. Wu (2009), Effect of the satellite laser ranging network distribution on geocenter motion estimation, *J. Geophys. Res.*, *114*, B04402, doi:10.1029/2008JB005727.

1. Background

[2] Analyses of Satellite Laser Ranging (SLR) tracking data have indicated for some years that the coordinate frame attached to the Earth's crust moves detectably relative to the Earth's total center of mass [*Eanes et al.*, 1997; *Bouillé et al.*, 2000; *Crétaux et al.*, 2002; *Moore and Wang*, 2003]. This translational motion is generally known as "geocenter motion." Apart from some measure of SLR technique errors, the bulk of the observed geocenter motion is thought to arise as a compensating response to the movements of planetary fluid masses (atmosphere, oceans, continental surface water, ice sheets, etc.), and presumably involves tidal, nontidal (mostly seasonal), and secular components [*Dong et al.*, 1997; *Chen et al.*, 1999]. Only surface fluid layers are expected to contribute significantly on timescales shorter than decadal, while mass motions deeper inside the Earth probably operate over longer intervals.

[3] To better understand the magnitude of geocenter motion and the ability of the satellite observing techniques to measure it, the International Earth Rotation and Reference Systems Service (IERS) conducted a focused analysis campaign in 1997–1998 [*Ray*, 1999]. The general impression at that time was that the net translation of terrestrial coordinate frames is detectable but small, probably less than 1 cm per component. The diurnal and semidiurnal tidal loading variations appeared to be well determined and in good agreement with modern ocean tidal models [*Watkins and Eanes*, 1997]. There was some overall agreement among the satellite techniques in detecting seasonal variations, but not enough to justify an operational IERS geocenter time series. Geophysical computations of the expected motions based on global fluid models were only very roughly consistent with the available geodetic observations a decade ago. The IERS currently recognizes geocenter motions in only limited ways, in some parts of its Conventions 2003 [*McCarthy and Petit*, 2004] and in the most recent realization of the International

[1] Laboratoire de Recherche en Géodésie, Institut Géographique National, Marne-La-Vallée, France.
[2] NOAA National Geodetic Survey, Silver Spring, Maryland, USA.
[3] Department of Physics and Material Sciences, University of Luxembourg, Luxembourg, Luxembourg.
[4] Jet Propulsion Laboratory, California Institute of Technology, Pasadena, California, USA.

0148-0227/09/2008JB005727$09.00

Terrestrial Reference Frame (ITRF), ITRF2005 [*Altamimi et al.*, 2007].

[4] It is worth noting the lack of any standardized expression for geocenter motion, including its sign or an exact method for its realization. We choose here to refer to geocenter motion as the net displacement of a frame whose origin coincides with the center of mass of the whole Earth system, CM (as realized ordinarily by observations of satellite orbits), with respect to the center of the figure of the Earth (CF). Our sign convention explicitly defines the geocenter as being the CM, as the term is commonly used in celestial mechanics. Such definition of geocenter motion is often adopted but its connection with the translation observations derived from space geodesy is only discussed in a qualitative way concerning SLR analysis. As stations are located on the Earth surface and estimated coordinates expressed with respect to the CM, the net translation of the geodetic network has always been interpreted as geocenter motion.

[5] Following the IERS campaign, studies have continued and the capabilities of the models and observing methods have improved. Beginning 27 February 2000, the International Global Navigation Satellite System Service (IGS) started to account explicitly for apparent geocenter motion in its Final GPS products [*Kouba et al.*, 1998; *Springer*, 2000]. Nevertheless, the observed translations using GPS have been described as "orbit parameters" more so than geophysical quantities due to strong correlations with the empirical solar radiation parameters that must also be adjusted in the data analyses [*Hugentobler et al.*, 2005]. Another method based on the theoretical modeling of the Earth's elastic response to a load is preferred using GPS results. Indeed, as described by *Blewitt et al.* [2001], the redistribution of terrestrial surface fluids that gives rise to geocenter motion should also be associated with changes in the lithospheric loading leading to deformations of the crust. They found that such deformation could be used to invert for degree-1 surface mass loading coefficients and the resulting geocenter motion. According to *Blewitt* [2003], their relationship is given by

$$T_{CM/CF} = \left(1 - \frac{1}{3}\left[h_1' + 2l_1'\right]_{CE}\right)\frac{4\pi R^3}{3M}\begin{pmatrix}\sigma_{11}^c\\ \sigma_{11}^s\\ \sigma_{10}^c\end{pmatrix}, \qquad (1)$$

where σ_{10}^c, σ_{11}^c, σ_{11}^s are the degree-1 coefficients of the fluid layer surface density developed as a spherical harmonic expansion. h_1' and l_1' are the load Love and Shida numbers, which can be computed from an Earth model centered on the solid component only (CE), R the mean radius and M the mass of the Earth. *Wu et al.* [2002, 2003] pointed out that a truncated degree-1 model is inadequate to represent the Earth's actual loading deformations; higher degree coefficients are needed for a realistic network distribution composed of 200 GPS stations. Further modeling refinements have been developed to improve geocenter motion estimates using such methods as: constraining load variability over the oceans [*Kusche and Schrama*, 2005]; using ocean bottom pressure (OBP) data over the oceans together with an increased number of GPS sites [*Wu et al.*, 2006]; using data from the Gravity Recovery and Climate Experiment (GRACE) in combination with GPS [*Davis et al.*, 2004; *Kusche and Schrama*, 2005; *Wu et al.*, 2006]; or using modified spherical harmonic expansions as basis functions to deal with the limited loading response of oceans and their sparse data coverage [*Clarke et al.*, 2007]. Such inversion methods, applied to GPS results, have been shown to produce more consistent geocenter motion time series among different Analysis Centers (ACs) than simple translation estimation [*Lavallée et al.*, 2006]. Note also that a new method proposed by *Swenson et al.* [2008] may be used to derive geocenter motion time series from GRACE results and an OBP model.

[6] It is worth mentioning that another often encountered definition of geocenter motion relates the CM to the center of mass of the solid Earth (CE) considered without its fluid layers [*Farrell*, 1972]. According to *Blewitt* [2003], the relative position between CE and CF is given by

$$\begin{aligned} T_{CF/CE} &= \left(\frac{1}{3}\left[h_1' + 2l_1'\right]_{CE}\right)\frac{4\pi R^3}{3M}\begin{pmatrix}\sigma_{11}^c\\ \sigma_{11}^s\\ \sigma_{10}^c\end{pmatrix} \\ &= \frac{\frac{1}{3}\left[h_1' + 2l_1'\right]_{CE}}{1 - \frac{1}{3}\left[h_1' + 2l_1'\right]_{CE}} \cdot T_{CM/CF} \\ &= -0.0206 \cdot T_{CM/CF}, \end{aligned} \qquad (2)$$

where the numerical values are computed using *Farrell* [1972] Love numbers. So as recognized by *Dong et al.* [1997], the vectors CF-CM and CE-CM are collinear and the magnitude of their difference is around 2%, which is about 0.1 mm. These two definitions are consistent within our current level of measurement accuracy but we prefer the first due to the practical geodetic realization of the network origin, as justified later. However, it should be mentioned that the IERS has started recommending ocean tide loading coefficients with optional geocenter corrections based on CM motion with respect to the CE frame.

[7] We will specifically study here the SLR technique and its ability to estimate the nonlinear variations of the geocenter motion as previously defined. Two distinct procedures are most often used to derive such estimates from SLR data. The first determines the degree-1 spherical harmonic coefficients of the gravity field, which are proportional to the geocenter motion. This method was used by *Devoti et al.* [1999] and *Pavlis* [1999] who both defined the reference frame by fixing coordinates for two stations. *Pavlis* [1999] has shown that this method gives consistent results with the second method, which estimates the net translational motion of the SLR tracking network whose coordinates refer to a quasi-instantaneous center-of-mass reference frame with respect to long-term linear positions (to account mostly for tectonic motions). The first published SLR results for geocenter motion were obtained by computing translational estimates directly from SLR range residuals [*Eanes et al.*, 1997; *Watkins and Eanes*, 1997; *Chen et al.*, 1999; *Cheng*, 1999]. Euclidian similarity parameters, the so-called Helmert parameters, were estimated in recent papers on SLR geocenter motion by *Bouillé et al.* [2000], *Crétaux et al.* [2002], and *Moore and Wang* [2003]. The translation estimation of these three analyses and those of *Chen et al.* [1999] are quite consistent at the annual frequency. Estimation of the scale of the SLR network (that is, its net radial variation) is usually considered only briefly and based on physical considerations rather than data analysis.

One should recall that all contributions to gravity or station displacement that are sufficiently accurately known are conventionally taken into account when processing SLR observations, including solid Earth tides, ocean loading and pole tides [*McCarthy and Petit*, 2004].

[8] During the past decade, comparison of SLR geocenter motion estimates with geophysical models has been regarded as a good opportunity to cross-validate the global reliability of both. *Chen et al.* [1999] made the first quantitative comparison of SLR results and a model based on fluid mass motions. The authors noticed the same order of magnitude and comparable seasonal signals in the two data sets although good consistency was not yet achieved. Some differences could clearly be seen between their geophysical model and prior results from the work of *Dong et al.* [1997], notably in the hydrological contribution; see the discussion by *Bouillé et al.* [2000]. *Bouillé et al.* [2000] and *Crétaux et al.* [2002] reached similar conclusions and interesting agreement in their geocenter results, depending on the geophysical data sets tested. *Dong et al.* [2003] did the first comparison of SLR observations with forward and inverse modeling of geocenter motion, and demonstrated the efficiency of inverse methods. At the same time, *Wu et al.* [2003] found statistical agreement at the annual frequency of their GPS inversion for geocenter motion and direct SLR estimates, but the standard deviation for their model was quite large. The inverse estimation was refined by *Wu et al.* [2006], who found agreement between their combined GPS/OBP inverse model and SLR at the millimeter level for seasonal amplitudes and for monthly phases, except for the semiannual Z component variation. Similarly *Lavallée et al.* [2006] found good agreement between SLR annual geocenter motion and GPS inversions using official products from five of six IGS ACs. Interannual variations have been discussed by *Chen et al.* [1999], *Crétaux et al.* [2002], and *Wu et al.* [2006], and recently modulation of the seasonal geocenter signals has been analyzed by *Feissel-Vernier et al.* [2006] using a running average filter.

[9] The previous comparisons that were realized using SLR results implicitly assumed that SLR estimated translations and geocenter motion are equivalent quantities. The connection between them will be discussed here based on the definition of geocenter motion previously introduced. Their difference, which depends on the SLR tracking geometrical configuration and availability, is called network effect. Its nonlinear part will be evaluated here using two distinct loading models. For that purpose, network translations will be derived from station displacements due to loading effects, including the degree-1 term and station displacement leakage. One may wonder if it is preferable to compare such series to SLR estimated translations instead of geocenter motion time series computed with equation (1). Or conversely if it is possible to mitigate the network effect so that SLR translations could be better regarded as geocenter motion.

2. Geocenter Motion From Translation

2.1. Estimation Model

[10] By fixing the Earth gravity field degree-1 coefficients to zero when processing SLR satellites orbits, it is possible to theoretically estimate the positions of the satellite tracking stations with respect to the CM. This procedure is actually set up to process SLR station positions on a weekly basis, which gives access to a quasi-instantaneous CM. The translations of such sets of positions are commonly estimated by comparing them with "static" coordinates from an external solution that accounts for tectonic motions. Such an external solution supplies station coordinates as piecewise linear functions of time, as is the case for the ITRF solutions. Helmert parameters are estimated for this comparison using this formula as observation equation

$$\forall i, \quad X^i(t_k^i) = X_c^i + (t_k^i - t_0)\dot{X}_c^i + T(t_k) + (\lambda(t_k)I + R(t_k))X_c^i, \tag{3}$$

where, for each station i of the SLR quasi-instantaneous solution k, $X^i(t_k^i)$ is the tridimensional Cartesian position vector (at epoch t_k^i). X_c^i and $\dot{X}_c^i$ are the position (at the reference epoch t_0) and velocity of station i supplied by the solution c. $T(t_k)$, $\lambda(t_k)$ and $R(t_k)$ are respectively the translation vector, the scale factor and the rotation matrix needed to transform the coordinates of the external frame at the mean epoch of the solution k into the frame of the individual input set k. $R(t_k)$ contained the three rotations r_x, r_y and r_z around the three axes and $T(t_k)$ contains the three origin components that are interpreted as the geocenter motion (rigorously their opposite according to our chosen sign convention).

[11] The parameters $T(t_k)$, $\lambda(t_k)$ and $R(t_k)$ are estimated by standard least squares using the full variance-covariance information supplied with the input solutions. For an optimal use of the covariance information, it is preferable to use input frames defined by means of minimum constraints. So if loosely constrained solutions are available, minimum constraints should be applied, for example, following *Altamimi et al.* [2002] to ensure that the covariance reflects in an optimal way the noise of the measurements [*Altamimi et al.*, 2003]. Thus the Helmert parameter estimates are weighted by the internal precision of each input position determination. Such estimated translations are usually called geocenter motion as estimated by the network shift approach [*Dong et al.*, 2003; *Lavallée et al.*, 2006].

[12] Nothing prevents estimating simultaneously the secular frame (X_c, $\dot{X}_c$) using equation (3) if time series of quasi-instantaneous frames are available; this is the approach we have chosen and which was used to build the ITRF2005 [*Altamimi et al.*, 2007; *Collilieux et al.*, 2007]. This procedure is called stacking of position time series. The normal equation of the least squares estimation built with such a model has a rank deficiency that can be rectified if the output secular frame is sufficiently defined. Minimum constraints or internal constraints can be applied to define the output frame [*Altamimi et al.*, 2007] without any overconstraint or distortion. We have chosen internal constraints to specify the origin and scale. This condition ensures that the origin of the estimated secular frame is the averaged origin of the quasi-instantaneous frames [*Altamimi et al.*, 2008]. In case of SLR analyses, that origin is theoretically the averaged center of mass of the whole Earth over the period of observation. It consequently yields detrended time series of the translation vector. The orientation of the estimated frame ($\hat{X}_c$, $\hat{\dot{X}}_c$) is defined by means of minimum constraints applied to a core network of the SLR stations. Note that every station has some influence on the Helmert parameters even if it is not included in the subnetwork constraint.

2.2. Ideal Case

[13] In order to interpret the physical significance of the estimated frame translations, we first consider the simplified case where only translations are estimated, at a single epoch, between a frame centered on the quasi-instantaneous CM and a secular reference frame $(X_c, \dot{X}_c)$ (coordinates as piecewise linear functions of time). Rotation and scale factor parameters will be omitted for now. The quasi-observations are also assumed to be equally weighted here and the number of stations is assumed to be constant with time. In that case, the partial derivative of the least squares cost function for the translation component j is

$$\sum_{i=1}^{n} \left({}_jX^i(t_k^i) - {}_j\hat{T}(t_k) - {}_jX_c^i - (t_k^i - t_0)\,{}_j\dot{X}_c^i \right) = 0, \qquad (4)$$

where n is the number of points and i the point index. To interpret the nature of the translation, we define a new frame $\tilde{X}$. The position of station i in that frame is defined at the epoch t_k by $\tilde{X}^i(t^i_k) = X^i(t^i_k) - \hat{T}(t_k)$. Using this notation and making the difference of equation (4) at two consecutive epochs, and dividing it by the number of points n, one gets

$$\frac{1}{n}\sum_{i=1}^{n} {}_j\tilde{X}^i(t_{k+1}) - \frac{1}{n}\sum_{i=1}^{n} {}_j\tilde{X}^i(t_k) = (t_{k+1} - t_k)\frac{1}{n}\sum_{i=1}^{n} {}_j\dot{X}_c^i, \qquad (5)$$

i.e.,

$${}_j\tilde{X}^{CN}(t_{k+1}) - {}_j\tilde{X}^{CN}(t_k) = (t_{k+1} - t_k)\,{}_j\dot{X}_c^{CN}. \qquad (6)$$

This relation gives the displacement of the equally weighted barycenter of the network in the frame $\tilde{X}$. This point has been called Center of Network (CN) in the geodetic literature [*Wu et al.*, 2002, 2003] so this terminology is used here. Equation (6) tells us that the CN drifts linearly in the $\tilde{X}$ frame and that this drift depends on the time evolution of the secular frame $(X_c, \dot{X}_c)$. Equation (6) only constrains the secular time evolution of the CN in the $\tilde{X}$ frame. Thus the estimated translations $\hat{T}(t_k)$ exhibit the same nonlinear variations as the CN-CM motion. If the secular frame is defined such that the sum of the velocities equals zero, and that the sum of positions is also zero at a given epoch, the CN coordinates in frame $\tilde{X}$ are then fixed to zero such that the $\tilde{X}$ frame has its origin fixed to the CN. In that case, the translations $\hat{T}(t_k)$ would reflect CN-CM motion. In our approach, the secular frame is defined by means of internal constraints. So the translation time series obtained with respect to the secular frame have zero mean and are detrended. As a consequence, the estimated translations can be interpreted as detrended quasi-instantaneous CN with respect to CM motion estimates (but see the discussion below about global bias and weight influence).

[14] More generally, in case of a well distributed network, CN is expected to be close to the barycenter of all the Earth surface points, the Earth Center of Figure (CF) whose position can be defined in any frame of origin O as

$$\vec{X}_{CF} = \frac{1}{S}\iint_S \vec{OM}\,dS, \qquad (7)$$

where M is any point of the Earth surface S. In the loading theory where CF has been introduced, this integration is realized over the whole surface of the deformed Earth [*Trupin et al.*, 1992; *Blewitt*, 2003], which is surrounded by a fluid layer that has null thickness. When dealing with the real Earth, the considered surface is the solid Earth topography including the area below the oceans. The CF is not accessible by any geodetic network which only covers the continental Earth crust to a certain extent. If the origin O is chosen as the CF, the time derivative of equation (7) stresses that there is no net translational surface displacement in the CF frame [*Blewitt*, 2003].

[15] The interest in using such an ideal point is that it is universal and does not depend on any particular sampling of the Earth surface as done by a real geodetic network. Its major advantage is that geocenter motion models can be computed rigorously from fluid data using equation (1). In practice, the CN of a sparse network could be located far from the CF. Moreover, the variations of position between CN and CF are hardly influenced by tectonic effects. Working with detrended translations makes it possible to neglect the inaccessible constant between CM and CF (as well as between CF and CN) and removes the linear tectonic variations. Thus CN-CM variations should be close to the CF-CM variations. As a consequence, the estimated translations from equation (3) approximate detrended CF with respect to CM motion. This argument justifies our adopted definition of geocenter motion.

2.3. Interpretation of the Translation Parameters

[16] In this section, we aim to decompose the translations estimated from equation (3) into a geocenter motion and error components. When applying equation (3), additional terms for scale and rotations are introduced compared to the development of the previous section. Input sets of positions are also weighted with the inverses of their variance-covariance matrices Σ. We will assume that SLR position vector X_{SLR} can be decomposed into two terms: the true position X_{CM}^{truth} expressed with respect to the CM and a noise and systematic error term Δ. The least squares estimation of the Helmert parameters $\hat{\theta}$ between X_{SLR} and the fixed secular frame $(X_c, \dot{X}_c)$ can be computed at a specific epoch t_k by

$$\hat{\theta} = \left(A^T\Sigma^{-1}A\right)^{-1}A^T\Sigma^{-1}\left(\left[X_{CM}^{truth} + \Delta\right] - X_c(t_k)\right), \qquad (8)$$

where

$$\hat{\theta} = \left[\hat{t}_x, \hat{t}_y, \hat{t}_z, \hat{\lambda}, \hat{r}_x, \hat{r}_y, \hat{r}_z\right]^T = \left[\hat{T}^T, \hat{\lambda}, \hat{r}_x, \hat{r}_y, \hat{r}_z\right]^T.$$

A is the partial derivative matrix derived from equation (3) that can be found, for example, in the work of *Altamimi et al.* [2003]. For clarity, the time argument t_k has been omitted, except for position $X_c(t_k) = X_c + \dot{X}_c(t_k - t_0)$. Equation (8) can be split into two parts

$$\begin{aligned}\hat{\theta} &= \left(A^T\Sigma^{-1}A\right)^{-1}A^T\Sigma^{-1}\left(X_{CM}^{truth} - X_c(t_k)\right) \\ &\quad + \left(A^T\Sigma^{-1}A\right)^{-1}A^T\Sigma^{-1}\Delta \\ \hat{\theta} &= \hat{\theta}_{c/CM} + \hat{\theta}_{\Delta}. \end{aligned} \qquad (9)$$

The second part of equation (9) corresponds to the error term. If we isolate the three first components of $\hat{\theta}$, that are the translations, we get from equation (9), keeping the two separated parts

$$\hat{T} = \hat{T}_{c/CM} + \hat{T}_{\Delta}. \tag{10}$$

Following the previous arguments concerning equations (4) to (6), the term $\hat{T}_{c/CM}$ can be decomposed into

$$\hat{T}_{c/CM} = \left[T_{c/CN} + T^{truth}_{CN/CM}\right] + \hat{\delta}_{w,c}. \tag{11}$$

where $T_{c/CN}$ is a linear function of time that carries the information of the frame definition of the adopted secular frame. Indeed, $(X_c, \dot{X}_c)$ does not have its origin at the SLR CN, see equation (6). $\hat{\delta}_{w,c}$ represents the error contribution due to the correlation effect between translation and other Helmert parameters, and the weighting. Note also that some part of station displacement may also have leaked into the rotation and scale estimates, not only the translations. $T^{truth}_{CN/CM}$ is the translation between the CN and CM frame defined by

$$T^{truth}_{CN/CM} = \frac{1}{n}\sum_i X^{truth,i}_{CM}. \tag{12}$$

Equation (11) does not isolate the geocenter motion term. So we define

$$\hat{T}_{net} = \hat{\delta}_{w,c} + T^{truth}_{CN/CF}, \tag{13}$$

as being the network effect term where $T^{truth}_{CN/CF}$ is the relative position of CN and CF. As it is, $\hat{T}_{net}$ defines the difference between the concept of geocenter motion and the way we actually realize it through the CN taking into account the uncertainty of the estimator. Then we can write

$$\hat{T}_{c/CM} = T_{c/CN} - T^{truth}_{CM/CF} + \hat{T}_{net}, \tag{14}$$

where $T^{truth}_{CM/CF}$ is the true value of the geocenter motion. And so adding the noise part, the estimated SLR translation is

$$\hat{T} = T_{c/CN} - T^{truth}_{CM/CF} + \hat{T}_{net} + \hat{T}_{\Delta}. \tag{15}$$

[17] Equation (15) decomposes in the most general way the estimated translation into various terms and so shows that geocenter motion $T^{truth}_{CM/CF}$ and translation estimates $\hat{T}$ are not exactly equal. The aim of the next part is to evaluate that difference.

3. Evaluation of the Network Effect

[18] Interpreting detrended SLR translations as detrended geocenter motion is erroneous. The issue is to know how large the difference is. If we have a consistent model of what X^{truth}_{CM} and $T^{truth}_{CM/CF}$ are, it is possible to evaluate the error we make when interpreting $\hat{T}$ as the geocenter motion. Indeed, equation (9) can be used to compute $\hat{T}_{c/CM}$ from X^{truth}_{CM}, which is similar to the SLR derived translation. Following equation (14) and our sign convention, the difference between estimated translation expectation and $T^{truth}_{CM/CF}$ is

$$\hat{T}_{c/CM} - \left(-T^{truth}_{CM/CF}\right) = \hat{T}_{net} + T_{c/CN}. \tag{16}$$

[19] We will evaluate further that error term using models that supply displacements in the CM frame due to loading for every station as well as a geocenter motion time series. By the nature of the loading models, local displacements are constrained by the geocenter motion information that is contained in the degree-1 coefficients. Here we consider loading geocenter motion models with bias and trend removed over the considered period. Moreover, when using internal constraints to define the frame translation time series, we choose a specific secular frame $(X_c, \dot{X}_c)$ so that the $\hat{T}_{c/CM}$ time series is detrended. As $T_{c/CN}$ of equation (16) is a linear drift, the dominant term is

$$\hat{T}^{loading}_{net} \approx \hat{T}^{load}_{c/CM} - \left(-T^{load}_{CM/CF}\right). \tag{17}$$

where $\hat{T}^{loading}_{net}$ is the detrended network effect due to loading. According to equation (13), this term mostly accounts for the difference of origin between CN and CF. It does not include any noise term.

[20] Two models of SLR station displacements caused by loading effects will be considered in the following to evaluate $\hat{T}^{load}_{c/CM}$ and so the network effect term. The averaged radial motion of the SLR network, $\hat{\lambda}_{c/CN}$, as derived from a model using equation (9) will be also evaluated. The first loading model that is used has been computed from an inversion of the surface density of the load that causes variations in GPS nonlinear position time series: it will be called inverse model or model A. The second model has been computed from fluid data and will be called forward model or model B. Until recently, these models consisted of the two more general classes of existing models for station displacement and geocenter motion. Geocenter motion can now be derived from GRACE data [*Swenson et al.*, 2008] and so a third class exists, but only for data starting in 2003. Conversely, the two models that we will use cover most of the SLR data history. The next two sections describe the adopted loading models that will be used thereafter.

3.1. Inverse Model A

[21] The first model has been built from GPS and OBP data at monthly intervals. It consists of spherical harmonic coefficients which represent the surface mass distribution up to degree and order 50, equivalent to a spatial resolution of 800 kilometers. These coefficients can be used to compute ground displacements in the quasi-instantaneous CM frame using load Love numbers [*Greff-Lefftz and Legros*, 1997] at any place in the world although the precision is not spatially uniform. The model coefficients have been estimated from approximately 450 monthly GPS position time series and from detrended OBP values derived from the Estimating the Circulation and Climate of the Ocean (ECCO) model for 1993 to 2006. Only relative GPS deformation measurements have been used in the inversion, in the form of three-dimensional detrended residual position time series obtained through Helmert parameter transformations.

[22] The ECCO model has been resampled and biases reflecting unknown water exchange with land have been estimated along with the surface mass coefficients as described by *Wu et al.* [2006]. As both GPS measured displacements and OBP data are linearly related to surface mass distribution spherical harmonics coefficients, the latter can be estimated by inversion. However, the spherical harmonic development needs to be truncated due to finite measurement number and distribution. Thus the inversion procedure is conducted using a regularization method controlled by the properties of the a priori geophysical fluid model that has been used.

[23] The model is estimated from detrended time series and so cannot reflect long-term trends in the surface mass distribution. This model includes degree-1 coefficients and so implicitly contains the geocenter motion. The degree-2 coefficients are shown to agree remarkably well with GRACE results [*Wu et al.*, 2006]. This model is also shown to contain significant interannual variations. As a consequence, it is interesting to check if they are also found in the geophysical fluid-based geocenter model and in the SLR results.

3.2. Forward Model B

[24] The forward model of station displacement is created using global geophysical fluid data convolved with mass loading Green's Functions [*Farrell*, 1972]. The method was first outlined in [*van Dam and Wahr*, 1987]. Only deviations from that method will be described here. The surface mass contributions include atmospheric pressure, continental water storage, and ocean bottom pressure.

[25] The input atmospheric pressure data is the National Center for Environmental Prediction surface pressure. This data is provided on a $2.5^\circ \times 2.5^\circ$ global grid at 6-hour intervals. We account for the pressure load over the ocean using the modified inverted barometer as described by *van Dam and Wahr* [1987]. The ocean-land mask has a resolution of 0.25° and is derived from ETOPO5 [*NOAA*, 1988].

[26] The continental water storage data comes from the *LaDWorld-Fraser* model. This is an update of the *LaDWorld-Amazon* model described by *Shmakin et al.* [2002] and *Milly and Shmakin* [2002]. The water storage load is provided on a $1.0^\circ \times 1.0^\circ$ global grid at monthly intervals. We do not include storage effects over the Arctic and Antarctic regions as the model does not model the glacier dynamics in these regions well.

[27] The ocean bottom pressure is derived from the ECCO model provided on a $1.0^\circ \times 1.0^\circ$ grid at 12 hourly intervals [*JPL*, 2008].

[28] For the forward model, we begin by generating a time series of three-dimensional surface displacements for each station and each surface pressure component. We convolve each surface load with Farrel's Green's functions [*Farrell*, 1972] which have been computed in the CM frame [*Blewitt*, 2003] corresponding to the SLR reference frame. At this point, there are three separate time series for each station which represent the contributions from the individual surface loads. For the 6 hourly atmospheric pressure and the 12 hourly ocean bottom pressure, we average the results into a weekly estimate at the central epoch of the GPS week. We interpolate the monthly water storage data into weekly estimates using a cubic spline. Finally we combine the three separate series into a single series following the approach of *Clarke et al.* [2005].

[29] It is worth noting that this model is not completely independent of the inverse model as both incorporate the same ocean bottom pressure data.

3.3. Modeling of Translational and Radial Motions

[30] We wish to build model translations $\hat{T}_{c/CM}$ and scales $\hat{\lambda}_{c/CN}$ from the two loading models. To compute those terms, we need a reference set of SLR stations at every epoch. We use as a reference the SLR position time series which were submitted for ITRF2005 analysis from 1993.0 to 2006.0 by the International Laser Ranging Service (ILRS) Analysis Working Group (AWG). The SLR network for that period is composed of 87 stations. Not all of them observed continuously. In fact, most of them operated occasionally or for limited time periods. On average, 20 stations are used on a typical week. For ITRF2005, five ACs contributed weekly time series solutions for station positions and daily Earth Orientation Parameters (EOPs) based on fits for the orbits of the LAGEOS 1 and 2 geodetic satellites. A weekly combined ILRS solution has been generated at Agenzia Spatiale Italiana (ASI); details of the combination procedure can be found in the work of *Luceri and Pavlis* [2006]. The full variance-covariance matrices of the adjusted parameters are also provided.

[31] In order to compute the translations $\hat{T}_{c/CM}$, we need to know the position of every SLR station with respect to the CM. So the synthetic position time series $X^{truth}_{CM}(t_k)$, denoted $X^{load}_{CM}(t_k)$, have been generated from the loading models at every epoch of the SLR data set, only for the SLR stations available at that epoch for the period 1993.0 to 2006.0. The position of station i at epoch t_k is computed as

$$X^{load,i}_{CM}(t_k) = X^{i}_{ITRF2005}(t_k) + \Delta X^{load,i}_{CM}(t_k), \tag{18}$$

where $X^{i}_{ITRF2005}(t_k)$ is the ITRF2005 coordinates of station i at the epoch t_k and $\Delta X^{load,i}_{CM}(t_k)$ is the displacement of the station in the CM frame as supplied by each loading model. In a second step, the two synthetic time series $X^{load}_{CM}(t_k)$ are used as input to equation (9) to estimate the transformation term $\hat{\theta}_{c/CM}$. We employed the stacking procedure described in section 2.1 by estimating also the stacked frame. We use in that process the variance-covariance matrix of the corresponding ILRS position set at every epoch that is needed in equation (9). In order to avoid any bias in the stacked solution estimated in the second step, each station displacement model time series $\Delta X^{load,i}_{CM}(t_k)$ has been detrended beforehand.

[32] This operation is in fact very easy to implement by simply taking an SLR position solution, usually supplied in the SINEX format [*Blewitt et al.*, 1994] (see http://www.iers.org/MainDisp.csl?pid=190-1100110), and by replacing the estimated positions by synthetic positions computed using equation (18) without modifying the covariance matrix (to which minimum constraints have previously been applied). Then this file can be used as input to estimate the Helmert parameters with respect to a long-term solution using any available software that estimates Euclidian similarity parameters.

[33] As a product of this analysis, we get vector $\hat{\theta}^{load}_{c/CM}(t_k)$ at every epoch as well as its covariance matrix for the two models A and B. As the covariance of the model A is

provided, we choose to use it to estimate the covariance matrix of the Helmert parameters time series obtained from stacking, which was not possible with the previous described algorithm. The variance of this model decreases with time due to the gradually increasing number of GPS stations available to the inverse model. Our procedure is to replace the covariance matrix with a covariance matrix computed as described in Appendix A using the full covariances of the displacements $\Delta X^i_{CM}(t_k)$. Standard deviations for the three translations decrease with time from 1.5 mm to 0.6 mm, on average, and for scale are about 0.6 mm. These values are higher than the formal errors estimated by the stacking of the ILRS simulated time series.

[34] Note that we did not include a noise term $\Delta(t_k)$ in equation (18) since we are not primarily interested in evaluating conjointly the term $\hat{T}_\Delta$ of equation (15). We have evaluated it independently using SLR covariance matrix time series. One thousand time series of the vector $\hat{T}_\Delta$ have been generated from realizations of SLR Gaussian spatially correlated noise Δ used as input to equation (9). Median WRMS values of 2.0 mm and 2.4 mm have been evaluated for each equatorial component and for Z component respectively.

3.4. Network Effect Magnitude

[35] We evaluate in this section the network effect term $\hat{T}^{loading}_{net}$ of equation (17) using the two previously introduced loading models. The issue of the origin of SLR scale temporal variations will be discussed in part 4.4 for evaluation of the model accuracy. Here we mention the order of magnitude of the rotation from the estimated vector $\hat{\theta}^{load}_{c/CM}(t_k)$ since they will not be discussed in more details in the following. For both model A and B, the estimated rotations are rather small although larger rotations are estimated about the Y axis. The scatter is at the level of one millimeter or less for all three components for both models.

[36] Figure 1 shows the network effect $\hat{T}^{loading}_{net}$ evaluated from the two models for the whole period of time. It mostly consists of high-frequency variations superimposed on seasonal terms. The scatter and seasonal sinusoidal signals of the network effect estimations are shown in Table 1. We find that the magnitude of the SLR network effect is less than two millimeters for the three components. These values are higher than those predicted by *Wu et al.* [2002] who had evaluated the network effect at the level of one millimeter for the SLR network. However, they had neglected the weighting and the influence of the estimation of rotations and scale. The Y component seems less affected than the others. Annual signal amplitudes are higher than 1 mm for the X and Z component and both loading models predict roughly consistent annual phases. As a consequence, the network effect probably influences any interpretation of the translations at the annual period. However, the semiannual network effect contributions are only marginally significant and not consistent between the two models.

[37] The network effect derived from model B is quite stable and does not show drastic interannual variations. It is an indicator of the lesser geometric influence of the network on the Helmert parameter estimates. However, this interpretation should be taken with caution when considering real data since the SLR network geometry affects these results in two distinct ways. First, the strength of the tracking network geometry is fundamental in determining all the correlated geodetic parameters and above all the satellite orbits. Second, the network distribution influences the Helmert parameters estimates. Here we see that the second effect is not so significant since it is not responsible for interannual variations.

4. Methodology for Comparing a Loading Model to SLR Translations

[38] SLR translations are usually compared to a loading model using the geocenter motion time series $-T^{load}_{CM/CF}$. However, the network effect magnitudes in Table 1 are significant compared with the geocenter motion magnitude. We suggest to compare SLR translations with the translations $\hat{T}^{load}_{c/CM}$ derived from the two loading models instead of their negative geocenter motions $-T^{load}_{CM/CF}$ and ask if the agreement between SLR translations and loading models improves with that approach. When doing so, we have to recognize that the loading models are not exact which means that the model noises contribute to the translation estimates $\hat{T}^{load}_{c/CM}$. In the following, to avoid confusion, $T^{load}_{CM/CF}$ will be called geocenter motion model and $\hat{T}^{load}_{c/CM}$ translation model.

4.1. Compare Translation Variations From Models and SLR Observations

[39] SLR frame translations derived from the ILRS solution fluctuate within 1 cm at weekly samplings. They are dominated primarily by white noise for periods shorter than roughly two months. As mentioned by *Bouillé et al.* [2000], the precision of SLR Z component estimates is poorer than the equatorial components by a factor 1.5, on average, due to concentration of the SLR stations in the northern hemisphere.

[40] Figure 2 shows the SLR translation time series, in black, with a running average filter of 10 weeks incorporated to suppress the dominantly white high-frequency noise. In order to test the effect of correlations in the simultaneous estimation of Helmert translation and scale parameters, Figure 2 also shows the ILRS translations when scale is not adjusted (gray line). Differences are usually so small that they are only occasionally and sporadically visible in the plot, mostly in the earlier years. Even though the SLR tracking network geometry is less than ideal, it is evidently adequate to justify the simultaneous estimation of scale in the standard stacking procedures (identical to the one used for ITRF2005). Translation $\hat{T}^{load}_{c/CM}$ derived from model A and B are plotted over in blue and red respectively, filtered in the same way. One can observe a strong similarity between the models and the SLR measurements, as well as between the two models themselves.

[41] Model B exhibits little interannual variation although the annual pattern varies considerably from year to year. Further, its scatter is quite stable. Greater interannual variations are contained in the ILRS and model A translations. The latter is less well determined in the earliest data due to poorer quality and sparser GPS data, as seen particularly in the Z component behavior. Model B is generally consistent in quality over the entire time period as improvements to the surface load models are applied over the entire data time span. The low-frequency agreement between the ILRS and model A translations is notably striking in the X component. We also see very general agreement of the annual patterns for all three time series and for all three components, but the pattern is not consistent at all observing times.

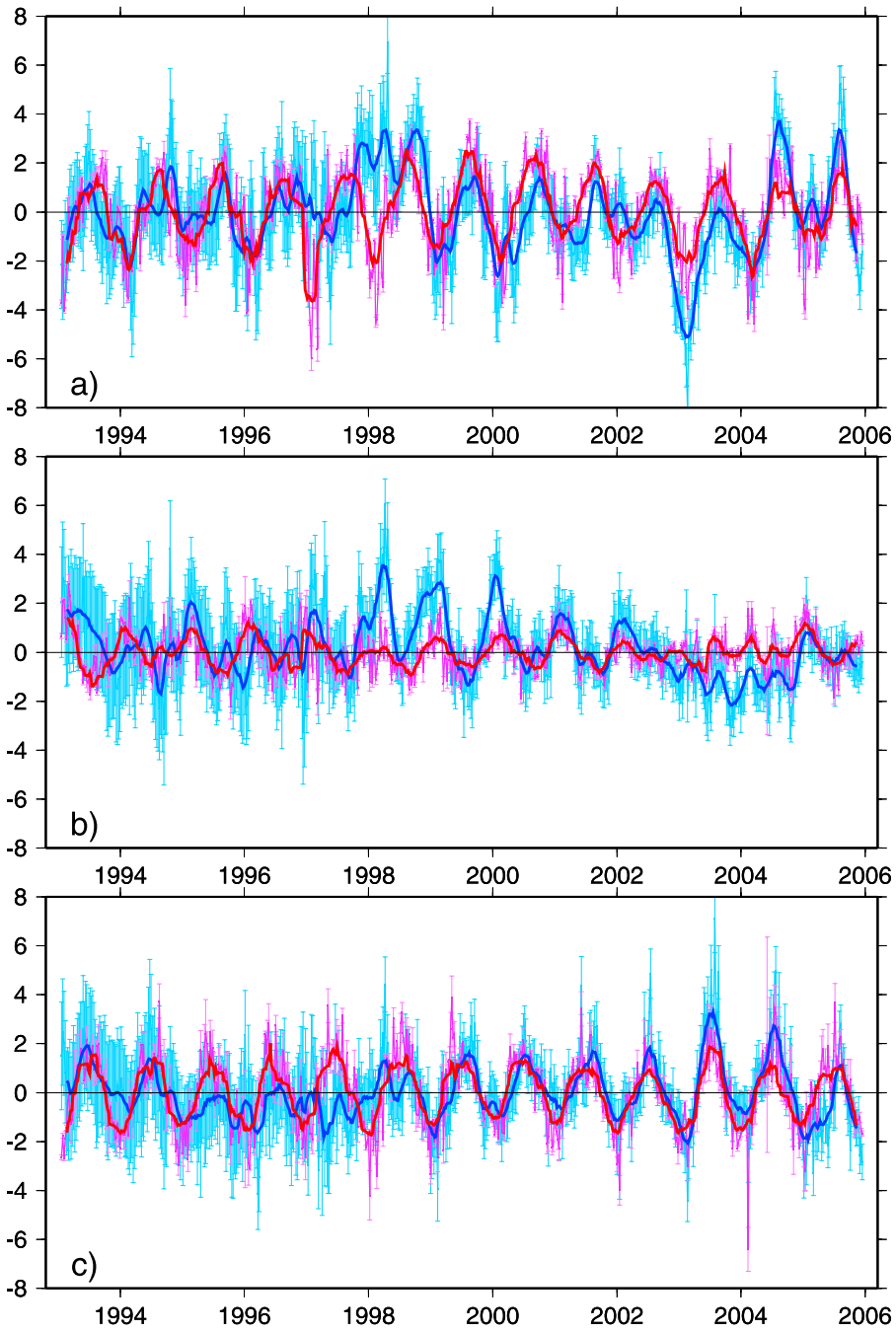

Figure 1. Network effect for translations in millimeters as a function of time: (a) X component, (b) Y component, (c) Z component. Light blue, model A; blue, model A with a 10-week running average filter applied; pink, model B; red, model B with a 10-week running average filter applied.

Table 1. WRMS and Seasonal Signals of the Network Effect Term for the Period 1993–2006 Derived From Two Loading Models[a]

			Annual		Semiannual	
	Loading Model	WRMS (mm)	A (mm)	ϕ (°)	A (mm)	ϕ (°)
X	A	1.9	1.3 ± 0.1	236 ± 4	0.4 ± 0.1	105 ± 11
	B	1.6	1.7 ± 0.1	225 ± 2	0.1 ± 0.1	205 ± 30
Y	A	1.3	0.7 ± 0.1	46 ± 5	0.3 ± 0.1	103 ± 10
	B	0.7	0.6 ± 0.1	40 ± 3	0.2 ± 0.1	68 ± 10
Z	A	1.4	1.2 ± 0.1	199 ± 3	0.3 ± 0.1	43 ± 12
	B	1.2	1.3 ± 0.1	178 ± 1	0.2 ± 0.1	197 ± 9

[a]The convention for the phase is $A\cos(2\pi f(t - 2000.0) - \phi)$, with t expressed in years and the frequency f in cycles/a.

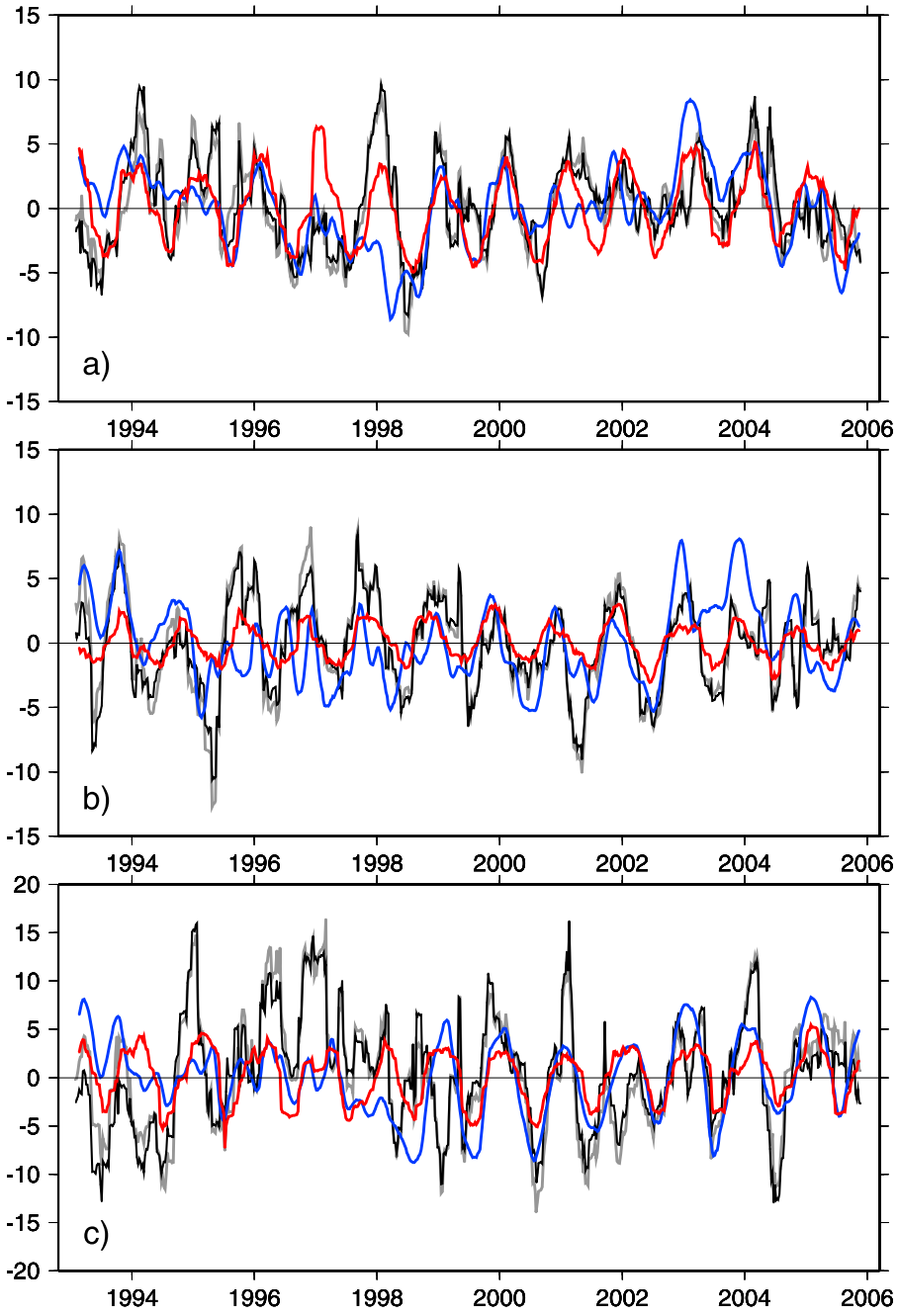

Figure 2. Estimated SLR translations smoothed with a 10-week running average filter (in millimeters): (a) *X* component, (b) *Y* component, (c) *Z* component. Black, ILRS with respect to ILRS long-term stacked solution; gray, ILRS with respect to ILRS long-term stacked solution but scale not estimated; blue, translation model from model A; red, translation model from model B.

[42] Cross-coherence analysis conducted between nonfiltered SLR translations and translation models mostly reveals consistency at the annual period for all three components and at the semiannual period for the *Z* component. The same conclusion could be reached when comparing SLR translations with the two respective geocenter motion time series. So no obvious better consistency is observed when dealing with translation model instead of geocenter motion. This confirms the previous analysis of the network effect time series themselves, which exhibit mostly annual variations. In the following, we consequently restrict our analysis to the frequency visibly coherent for all three components, i.e., the annual frequency. We also include the semiannual term for comparison with previous studies.

4.2. Seasonal Signals in the Translations

[43] The annual and semiannual waves fitted by weighted least squares are shown in Table 2 for translation time series. For the ILRS series, two versions are included. The top row for each component gives results when the scale parameter is estimated, and the second row when no Helmert scale parameter is adjusted with the translations. None of the ILRS

Table 2. Fits for Annual and Semiannual Variations and WRMS Residuals of SLR Translations and Scale Estimated for 1993.00–2006.0[a]

					Annual		Semiannual	
			WRMS (mm)	ILRS WRMS wrt. (mm)	A (mm)	ϕ (°)	A (mm)	ϕ (°)
X	$-\hat{T}^{SLR}$	ILRS	5.3	–	2.8 ± 0.3	41 ± 5	1.0 ± 0.3	351 ± 14
		ILRS ns	5.4	1.3	2.7 ± 0.3	45 ± 6	1.1 ± 0.3	2 ± 14
	$-\hat{T}^{load}_{c/CM}$	model A	3.6	5.1	2.4 ± 0.2	32 ± 4	0.8 ± 0.2	287 ± 13
		model B	3.1	4.6	3.7 ± 0.1	34 ± 2	0.1 ± 0.1	142 ± 73
	$T^{load}_{CM/CF}$	model A	2.4	4.9	1.3 ± 0.2	357 ± 10	0.7 ± 0.2	278 ± 21
		model B	1.8	4.5	2.0 ± 0.1	27 ± 2	0.1 ± 0.1	232 ± 37
Y	$-\hat{T}^{SLR}$	ILRS	5.3	–	3.5 ± 0.2	332 ± 4	0.6 ± 0.2	354 ± 20
		ILRS ns	5.7	1.2	3.8 ± 0.2	327 ± 4	0.8 ± 0.2	345 ± 17
	$-\hat{T}^{load}_{c/CM}$	model A	3.5	5.2	2.6 ± 0.1	322 ± 3	0.9 ± 0.2	265 ± 10
		model B	1.7	4.8	1.8 ± 0.1	324 ± 2	0.4 ± 0.1	203 ± 9
	$T^{load}_{CM/CF}$	model A	3.1	5.0	2.7 ± 0.3	336 ± 6	0.8 ± 0.3	269 ± 20
		model B	1.7	4.5	2.0 ± 0.1	338 ± 1	0.4 ± 0.1	180 ± 8
Z	$-\hat{T}^{SLR}$	ILRS	8.4	–	2.2 ± 0.4	352 ± 10	1.7 ± 0.4	187 ± 12
		ILRS ns	8.7	1.9	3.6 ± 0.4	4 ± 7	1.2 ± 0.4	188 ± 18
	$-\hat{T}^{load}_{c/CM}$	model A	4.8	8.1	5.3 ± 0.2	23 ± 2	0.7 ± 0.1	206 ± 13
		model B	3.1	8.1	3.7 ± 0.1	34 ± 1	1.0 ± 0.1	206 ± 5
	$T^{load}_{CM/CF}$	model A	3.8	7.9	4.0 ± 0.3	26 ± 4	0.3 ± 0.3	194 ± 49
		model B	2.8	8.0	2.8 ± 0.1	51 ± 2	1.4 ± 0.1	206 ± 4
Scale	$\hat{\lambda}^{SLR}$	ILRS	4.5	–	1.7 ± 0.2	214 ± 8	0.7 ± 0.2	3 ± 17
	$\hat{\lambda}^{load}_{c/CM}$	model A	1.3	4.5	0.6 ± 0.1	217 ± 6	0.4 ±0 .1	9 ± 10
		model B	1.0	4.3	1.0 ± 0.1	215 ± 3	0.0 ± 0.1	302 ± 52

[a]Same results for translation and scale models from two geophysical models are also presented. The second column gives the adopted sign convention, which is here consistent with our definition of geocenter motion. $\hat{T}_{c/CM}{}^{load}$ is the translation model estimated with the loading models and $\hat{\lambda}^{load}_{c/CM}$ the averaged radial motion, whereas $T^{load}_{CM/CF}$ is the loading model geocenter motion time series. ''ILRS'' refers to SLR results from 1993.0 to 2006.0 when all the Helmert parameters are estimated; ''ILRS ns'' indicates the solution when no scale parameter is adjusted along with the translational parameters. The convention for the phase is $A\cos(2\pi f(t-2000.0)-\phi)$ with t expressed in years and the frequency f in cycles/a.

fit results is significantly different at the two-sigma level except for the Z component annual amplitude. We choose to keep the fit obtained when the scale is estimated as the reference time series. The X component annual signals are very consistent for the ILRS and the two loading translation model time series $-\hat{T}^{load}_{c/CM}$, within two sigmas for the phase and the amplitude. The agreement in phase is also very good for the Y component although the amplitudes differ significantly. The ILRS annual Y translations are larger than either geophysical model. There might be a marginally significant phase advance of 20 to 40 degrees for the ILRS annual Z component compared to the models. The semiannual variations are all small, barely detectable, but the amplitudes and phases agree remarkably well among SLR observations and models for the Z component.

[44] Table 2 also presents the seasonal fit of the geocenter motion time series $T^{load}_{CM/CF}$ derived from the two loading models. They are consistent with each other at the 3 sigma level for the equatorial components. However, they slightly disagree for the Z component since a significant phase shift of about one month is observed. Differences between $T^{load}_{CM/CF}$ and $-\hat{T}^{load}_{c/CM}$, see Table 2, have to be attributed to the network effect. At the annual frequency, both loading models predict the same impact of the network effect. An increase in amplitude of about one millimeter in the X and Z components is observed, the Y component being unaffected. We note that the model translations are more consistent with the ILRS translation for the X component but not for the Z component. Both models confirm a phase shift of the annual signal of about seven days to one month for the X component if the translation models are considered instead of geocenter motion time series. Also in the Z component, the annual signal phase of the model B translation is closer to the ILRS observations than the geocenter model. Finally we note that the semiannual agreement is not significantly improved when comparing translation model instead of geocenter motion model with the ILRS translations results, except in the Z component according to the model B. It therefore seems that the translations $\hat{T}^{load}_{c/CM}$ derived from the loading models generally agree better at the seasonal frequencies with the ILRS translations than do the geocenter motion themselves.

4.3. Variance Analysis of the Translations

[45] To provide a perspective on the consistency of the ILRS translations and loading translation models at nonseasonal periods, we have also examined Weighted Root Mean Scatter (WRMS) changes with time. If we consider that an error term T^{load}_{Δ} also exists in loading model translations and that the network effect terms between SLR data and models are very nearly identical, we should have

$$Var\left(\hat{T}^{SLR}-\hat{T}^{load}\right)\approx Var\left(T^{SLR}_{\Delta}+T^{load}_{\Delta}\right). \tag{19}$$

As a consequence, if the model errors are small or relatively constant, then temporal changes in $Var(\hat{T}^{SLR}-\hat{T}^{load})$ should reflect mostly fluctuations in the SLR data quality. The impact of purely network effects on this metric should be limited. We test this assumption in the following. Figure 3 shows the weighted scatter of the ILRS nonfiltered translation time series for sliding overlapping windows of one year, as well as the percentage of WRMS reduction of the ILRS translations corrected by the model A translation, Figures 3a, 3b, and 3c, and by the model B translation, Figures 3a', 3b',

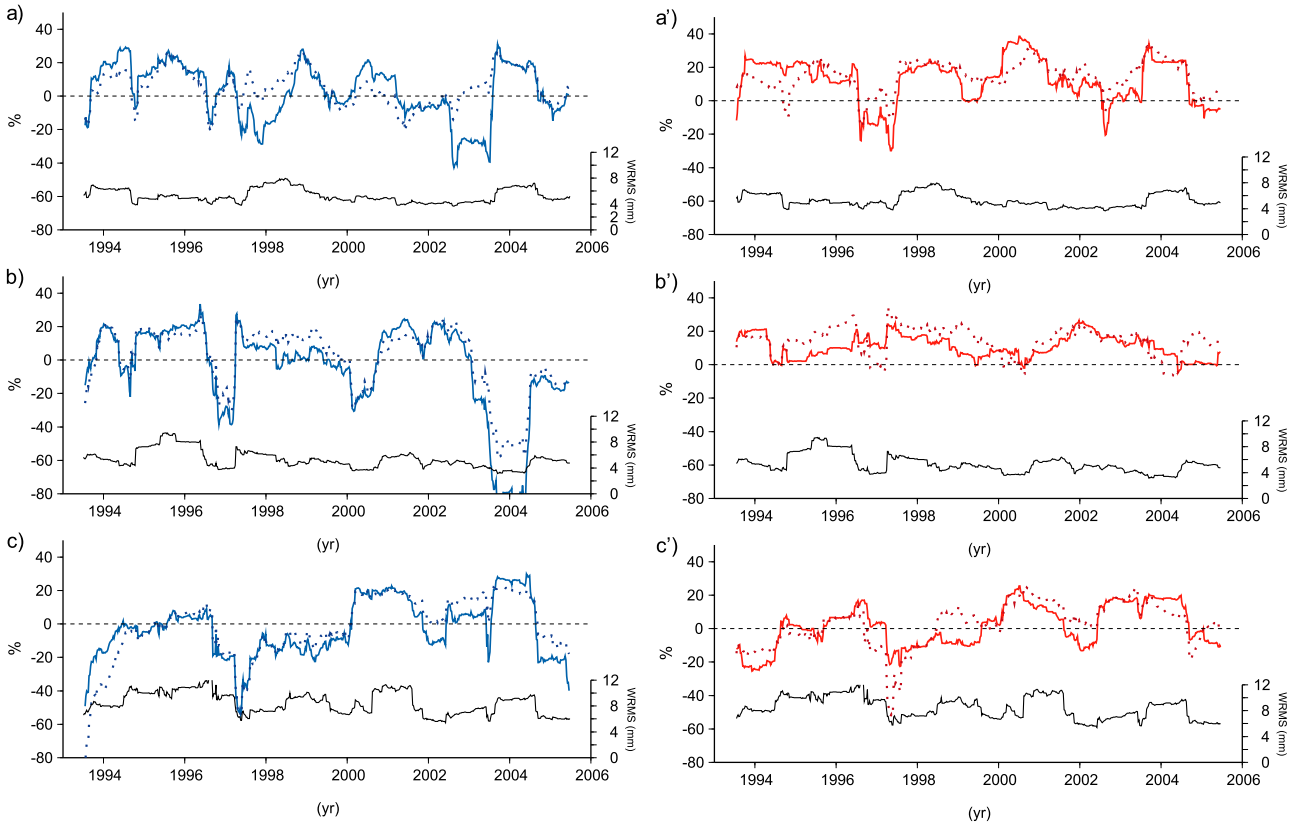

Figure 3. Percentage of WRMS reduction of ILRS translation time series computed for annual sliding windows using translation models (solid lines) versus using geocenter motion models (dash lines). Model A used for (a) *X* component, (b) Y component, and (c) *Z* component. Model B used for (a') *X* component, (b') *Y* component, and (c) *Z* component. Bottom solid black lines show the ILRS weighted scatters computed for annual sliding windows.

and 3c'. See Appendix B for the definition of percentage of WRMS reduction.

[46] Overall, the variance of the ILRS translations is much greater in the *Z* component than either equatorial direction. The translation models usually reduce the ILRS *X* and *Y* variances during most intervals. We note that generally model B is more effective for the *X* component, especially around 1998 and 2003–2004. The same would be true for *Y* as well, except for the period around 1995–1996 when model A is better. Model A itself seems to introduce excess variance in *X* around 1998 and 2003 and in *Y* during 1997, 2000, and 2003–2004. For the *Z* component, both models (especially the inverse model) account for the observed variance better after 2000. An explanation could be that the Hartebeesthoek station in South Africa started observing in 2000, thereby markedly improving the quality of SLR geodetic products due to the better network coverage. It seems however that ILRS *Z* translation variation is not well explained by the models around 2002.

[47] Figure 3 also shows the percentage of WRMS reduction when using geocenter motion models instead of translation models. In that case, network effect is left in the SLR corrected time series. The first comment is that the general pattern of the WRMS reduction is similar for the translation models and geocenter motion models in all cases. The geocenter motion models even explain slightly better the ILRS result at the intra-annual timescales since the variance reduction is generally higher when correcting SLR translation with geocenter motion models. Table 2 shows the WRMS of SLR translation corrected either by the translation models or the geocenter motion models, computed for the whole period of time. Using the geocenter motion models slightly reduces the WRMS for the three components compared to their translation models. This could imply that the network effect is not a major error source compared to the SLR solution noise.

[48] To conclude the translation study, the network effect magnitude due to loading is shown to be at the level of 1.5 mm RMS for the *X* and *Y* components but lower for the *Y* component. We have observed that the network effect impacts the translations at the annual timescale by about one millimeter for the *X* and *Z* components. It could be responsible of a shift of about seven days to one month for the *X* and *Z* component annual signals depending on the model. Although it is statistically significant, its effect on the interpretation of the translation as geocenter motion is limited since it does not create clear discrepancies between SLR translations and geocenter motion models. We have also noticed that the general high-frequency scatter of the SLR translations is not well explained by the network effect related to the surface loads.

4.4. Compare Scale Variations From Models and SLR Observations

[49] The estimation of the Helmert scale parameter has been mentioned as a critical issue for geocenter consideration

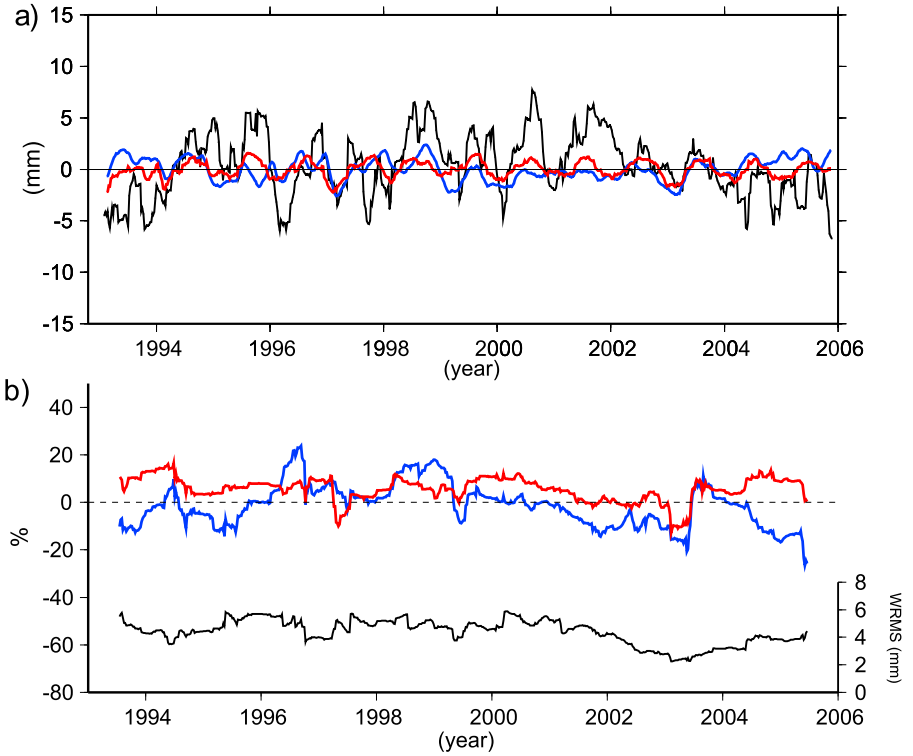

Figure 4. (a) Scale variations in millimeters smoothed with a 10-week weighted running-average filter. Black, ILRS with respect to long-term ILRS stacked solution; red, model B; blue, model A. (b) Percentage of WRMS reduction of ILRS scale time series computed for annual sliding windows using model A (blue) and model B (red). Bottom solid black line shows the ILRS weighted scale scatter computed for annual sliding windows.

in the case of GPS networks [*Lavallée et al.*, 2006; *Wu et al.*, 2006]. For SLR analysis, some authors have estimated the scale parameter, such as *Bouillé et al.* [2000] and *Crétaux et al.* [2002], whereas *Moore and Wang* [2003] did not. In the case of ILRS data analysis, as we have seen, estimating scale or not changes only the translation annual signal amplitude of the *Z* component. More important is that estimating the scale or not has a significant impact on the residual time series of station positions, which has consequences for their interpretation as physical site motions. However, *Altamimi et al.* [2007] have observed significant interannual and annual signals in the ILRS scale parameters from ITRF2005 suggesting that the scale estimates contain information from the ground motion. We wish to check if loading signals may be responsible, in part, for these variations. Conversely it could help validate the loading models that we have chosen.

[50] Figure 4a plots the ILRS scale parameters as well as scale effects estimated from the two geophysical models. The time series have been filtered using a 10-week running average for better viewing. The scatter of the ILRS scale is greater than for the models, but all show significant variations. These variations are an illustration of the effect of limited network sampling because there is no intrinsic scale bias in the geophysical models used to form the synthetic data. Both scale models are generally less scattered than the ILRS observations. Moreover, they do not match the slow decrease of the ILRS scale after 2002. The scale variations are smoother and larger in the model B compared to the model A. This might be due to the inherently lower spatial resolution of the inverse method (about 800 km) compared to the forward model B, which involves a loading convolution at the exact position of each station. The adjustment of scale parameters in the estimation process of model A might also explain the difference.

[51] Seasonal scale fits have been computed and given in Table 2. The ILRS scale annual signal amplitude is 1.7 ± 0.2 mm and the semiannual signal is 0.7 ± 0.2 mm. The model A scale semiannual variations are consistent at the 2 sigma level in amplitude and phase but the annual amplitude is 3 times smaller. Although model B does not contain a semiannual signal, the agreement of the annual signal amplitude with the ILRS annual scale is better with a value of 1.0 ± 0.1 mm and a consistent phase. As a consequence, most of the ILRS scale annual variations are probably due to loading effects.

[52] As with the translations, we conducted a similar variance analysis for the scale changes. In theory, if the models used for SLR data reduction were perfect, the scale parameter would be constant. So the detrended estimated scale parameter may be decomposed into two contributions: the noise from the term $\hat{\theta}_{\Delta}$ of equation (9) and the network effect term due to the average radial motion of the SLR network. Assuming that the network effect term of the SLR scale and of the model scale are identical, the variance of scale parameter differences is then given by

$$Var\left(\lambda^{SLR} - \lambda^{load}\right) \approx Var\left(\lambda_{\Delta}^{SLR} + \lambda_{\Delta}^{load}\right). \tag{20}$$

[53] Figure 4b shows that the annual variance of the ILRS scale can be partly explained by the model B scale. The

variability of the scale depends on the height determination of each site and is consequently sensitive to any radial error. It seems likely that SLR technique height errors are important, judging from the higher ILRS variability in Figure 4a. Any measurement error or bias affecting the SLR ranges could influence the scale parameters.

[54] We have shown here that the sinusoidal annual signal in this parameter is probably related to the nonmodeled loading effects. This gives us good confidence in our model. However, we cannot explain the behavior at other frequencies. This reinforces the conclusion by *Coulot et al.* [2008] who have attributed some of these variations to SLR instrumental range biases. The relevant parameters to estimate in that case are the station range biases. However, analyzing the estimated scale parameter is a quick way to qualify a frame time series and can be used to detect problems. We advise continuing the estimation of this parameter for reference frame analysis.

5. An Alternative Approach: Network Effect Handling

[55] In section 4.2 we have shown that the translation models derived from loading models agree generally better with SLR translations at the annual frequency, compared to geocenter motion model. However, the building of these translations requires full global loading models, not only the degree-1 components. An alternative approach would be to decrease the network effect to make the SLR translations more consistent with geocenter motion.

[56] This can only be done by introducing external independent observations. If we have an idea of what the ground motion should be, we can reduce the network effect. Thus we extend the equation (3) model to

$$\forall i, \quad X^i(t_k^i) = X_c^i + (t_k^i - t_0)\dot{X}_c^i + \Delta X^i(t_k^i) + T(t_k) + (\lambda(t_k) \cdot I + R(t_k)) \cdot (X_c^i + \Delta X^i(t_k^i)), \tag{21}$$

where $\Delta X^i(t_k^i)$ are new parameters, called displacement parameters, which model residuals to the linear position evolution. These parameters can be seen as the displacement of the station in a CF frame whose tectonic motions are already accounted for. If we assume that the translation $T(t_k)$ is an estimation of the nonsecular CN-CM translations according to equations (10) and (11), the displacement parameters represent approximately the detrended coordinate residuals with respect to the CN frame. If we have a knowledge of the displacements in the CF frame, we could bring the translation $T(t_k)$ back to the CF frame instead of the CN.

[57] Equation (21) is introduced so that the two frames $X(t)$ and $X_c(t) + \Delta X(t)$ have similar shape, i.e., the same geometrical invariants. It also makes explicit the problem of correlation that exists between the Helmert parameters, notably translations, and the station displacements. In the following, the long-term frame $(X_c, \dot{X}_c)$ is fixed to ITRF2005. Even with this simplification, the observation equation derived from equation (21) is rank deficient. Additional constraints are introduced as

$$\Delta X^i(t_k^i) = G \cdot \Delta E^i(t_k^i), \tag{22}$$

where G is the rotation matrix from a local to global frame and $\Delta E^i(t^i)$ is an external residual station motion estimate, expressed in the local frame.

[58] We adopt nonlinear residual positions estimated by GPS and derived from IGS combined solutions as values for the $\Delta E^i(t_k^i)$ terms. Indeed, the GPS tracking network covers most of the Earth surface so that GPS residual nonlinear positions should better approximate nonsecular residual positions with respect to a frame having CF as its origin. As a consequence, if the SLR displacement parameters are constrained to the GPS residual nonlinear positions, the estimated translation variation should exhibit GPS network CN with respect to CM variations. This argument is reliable only if SLR and GPS stations sense statistically equal ground motion at the colocated sites. This experiment should help check that assumption.

[59] Choosing GPS is not arbitrary because it is the geodetic technique that exhibits the best position repeatability. The ITRF2005 IGS position residual time series, computed by equation (21) would be a good candidate for displacement values. However, *Collilieux et al.* [2007] have also shown that using a well distributed IGS subnetwork to constrain Helmert parameters changes the residual estimates significantly: they differ by a scale factor that consists mainly of an annual term with one millimeter amplitude. As a consequence, we use two sets of GPS nonlinear residual positions as constraint values. One has been derived with the Helmert parameters computed for a well distributed IGS subnetwork, and the second is constituted by the ITRF2005 GPS position residuals, computed with the full IGS network.

[60] The IGS formal errors are used to weight the constraints. There is a difference of precision balance between horizontal and vertical components determined by GPS and SLR. The GPS weekly position formal errors are smaller for horizontals whereas SLR weekly formal errors are smaller for verticals. However, note that the SLR residual position time series WRMS values are at the same level for the two components [*Collilieux et al.*, 2007]. In order not to disturb the estimation of Helmert parameters, we choose to apply different variance factors for the horizontal and vertical constraints. A formal error factor of two for horizontals brings the GPS precision to the same level as SLR for those components. Conversely, according to the variance study of the ITRF2005 height residual time series by *Collilieux et al.* [2007], we divide the GPS formal height errors by a factor of four. SLR covariance matrices are left unchanged.

[61] Equations (21) and (22) have been used to estimate SLR Helmert parameters by weighted least squares for each week during the 1998.0–2006.0 period. Indeed, IGS position repeatability has improved significantly over that time. The estimated Helmert parameters have larger formal errors than those estimated without the displacement parameters. Moreover, they are correlated with the displacement parameters as expected. For example, the scale parameter is anticorrelated with the radial displacement parameters with an absolute maximum value of 0.6 averaged over the stations for the period 1998.0–2006.0.

[62] Statistics for the estimated Helmert parameters are shown in Table 3 for the two different sets of constraint values that can be compared to the Helmert parameters computed by equation (3), for the same period of time. The WRMS of the generated Helmert parameters is higher for the equatorial

Table 3. WRMS of Geocenter Motion (wrt. 0 Mean) Derived From the Two Loading Models and Seasonal Signals Estimated for 1998.00–2006.0[a]

				Annual		Semiannual	
			WRMS (mm)	A (mm)	ϕ (°)	A (mm)	ϕ (°)
X	$-\hat{T}^{SLR}$	ILRS	5.1	2.9 ± 0.3	48 ± 7	0.9 ± 0.4	34 ± 21
		ILRS + IGS full	5.6	2.8 ± 0.4	25 ± 7	0.9 ± 0.4	11 ± 22
		ILRS + IGS rest.	5.5	2.5 ± 0.4	19 ± 8	0.9 ± 0.4	18 ± 22
	$T^{load}_{CM/CF}$	model A	2.4	1.3 ± 0.3	6 ± 14	0.4 ± 0.3	273 ± 49
		model B	1.8	2.1 ± 0.1	28 ± 2	0.1 ± 0.1	137 ± 30
Y	$-\hat{T}^{SLR}$	ILRS	4.8	3.4 ± 0.3	338 ± 5	0.8 ± 0.3	4 ± 18
		ILRS + IGS full	5.2	3.3 ± 0.3	333 ± 6	0.3 ± 0.4	42 ± 58
		ILRS + IGS rest.	5.2	3.2 ± 0.3	327 ± 6	0.5 ± 0.3	42 ± 42
	$T^{load}_{CM/CF}$	model A	3.1	3.0 ± 0.3	338 ± 6	0.6 ± 0.3	250 ± 29
		model B	1.8	2.1 ± 0.1	338 ± 2	0.3 ± 0.1	184 ± 12
Z	$-\hat{T}^{SLR}$	ILRS	8.0	2.4 ± 0.4	1 ± 11	1.4 ± 0.4	176 ± 18
		ILRS + IGS full	7.6	3.7 ± 0.5	21 ± 7	2.1 ± 0.5	157 ± 13
		ILRS + IGS rest.	7.5	3.4 ± 0.5	17 ± 8	2.0 ± 0.5	154 ± 13
	$T^{load}_{CM/CF}$	model A	3.7	4.6 ± 0.2	23 ± 3	0.3 ± 0.2	194 ± 50
		model B	2.6	2.7 ± 0.1	48 ± 2	1.2 ± 0.1	209 ± 5
Scale	$\hat{\lambda}^{SLR}$	ILRS	4.3	1.7 ± 0.3	224 ± 8	0.3 ± 0.2	46 ± 47
		ILRS + IGS full	4.1	1.2 ± 0.2	237 ± 12	0.3 ± 0.2	2 ± 54
		ILRS + IGS rest.	4.1	0.6 ± 0.2	214 ± 24	0.1 ± 0.2	231 ± 120

[a]The first line for each parameter, called ILRS, shows the negatives of SLR translations from the standard approach as reference series for comparison. The second and third rows are: ILRS + IGS full: Helmert parameters estimated using equation (21) and (22) with contraints to the ITRF2005 IGS residuals. ILRS + IGS rest.: Helmert parameters estimated using equation (21) and (22) with contraints to the IGS position residuals computed with a restricted number of GPS sites (see section 5). The convention for the phase is $A\cos(2\pi f(t - 2000.0) - \phi)$ with t expressed in years and the frequency f in cycles/a.

translation components, but is lower for the Z component and for the scale factor compared with the standard approach. As GPS residual position time series are known to exhibit mostly seasonal signals [*Dong et al.*, 2002], we expect to see differences at those frequencies. We observe that the GPS constraint affects the annual scale estimates more than the annual geocenter translations. The scale parameter is probably the most relevant for this study. Using the IGS position residuals computed using a well distributed network makes the SLR scale annual signal smaller by a factor of two compared with using ITRF2005 IGS position residuals, but it is still significant with an amplitude of 0.6 ± 0.2 mm. However, both constraints decrease the SLR scale annual signal. This is an indication of two important results. First, using GPS to constrain the estimation of the Helmert parameters decreases the SLR scale annual signal. As no global radial bias is expected at this frequency, this means that the network effect has decreased. Second, it demonstrates that SLR and GPS sense approximately the same net radial motions because the scale signal observed in the standard approach is absorbed by the displacement parameters. Moreover, it indicates that the use of a well distributed GPS network is suitable for residual station position studies. The remaining annual scale signal could be due either to any additional scale bias in the GPS residual positions or to other SLR scale biases at the annual frequency.

[63] The ILRS seasonal translation signal is also significantly changed. The Z component annual and semiannual amplitudes increase compared to the standard approach. The amplitudes of the equatorial components are less affected. One may observe that the phase of the annual signal is shifted, especially for the X component. It is interesting to note that the agreement between the annual signal of the ILRS translation and geocenter motion model time series is much better with the new approach. Table 3 gives the statistics for the geocenter motion models for the same period of time. The annual signals of the translations agree at the three sigma level for the amplitude and phase with the geocenter motion models, except for the model B geocenter motion phase in Z. The agreement between SLR X and Z translation and loading model annual signals improves in phase when GPS data are used conjointly.

[64] The annual signals of the SLR translations and scale are modified when constraints are applied to decrease the network effect. These modifications are consistent with the differences observed between our two loading model translations and their respective geocenter motion. They consequently validate the previous conclusions obtained with models. They also give encouragement to combining SLR and GPS data to improve SLR geocenter motion estimates.

6. Discussions and Conclusions

[65] Geocenter motion is conventionally defined here to be the motion of the center of mass of the Earth (CM) with respect to the geometric center of the solid Earth surface (CF). SLR translations estimated between a quasi-instantaneous station position set, theoretically expressed with respect to the CM, and a secular reference frame are biased estimations of this phenomena. First, the sparseness of the network makes possible only to access the center of the SLR network CN which is distinct from the CF. Second, the estimation procedure that we use to determine this translation introduces a supplementary error term that comes from the weighting and correlations with rotation and scale parameters. Third, it is only possible to investigate SLR translational variations due to the inaccessible constant between CF and CM so they cannot be rigorously interpreted as geocenter motion. The difference is the network effect, which should be dominated at subdecadal timescales by loading signals.

[66] The network effect due to loading has been evaluated using two distinct and relatively independent loading models. Its magnitude is at the level of 1.5 mm RMS. It has been

shown that it could slightly shift the phase of the annual SLR geocenter motion estimate, by less than 1 month, and affect the X and Z annual geocenter motion amplitudes at the 1 mm level. It is worth mentioning that annual signals are significantly disturbed but not sufficiently to create clear discrepancies between SLR translation results and geocenter motion models, which could explain the rather good consistency obtained in previous SLR studies [*Chen et al.*, 1999; *Bouillé et al.*, 2000; *Crétaux et al.*, 2002; *Dong et al.*, 2003].

[67] Consequently, two approaches can be considered when comparing SLR geocenter motion results to a geophysical model. The first is to try limiting the network effect. We have succeeded in counterbalancing some part of it for ILRS data by adding additional constraints derived from GPS colocated station position residuals. The SLR scale annual signal has been mostly removed which implies a globally averaged good consistency between colocated ILRS and IGS heights. Translations have been modified so that the annual variations are more consistent with the loading geocenter motion models. The second approach consists of producing the load displacements at all SLR stations, which requires a full global loading model, not just the degree-1 terms. We have shown that when doing so, the agreement between SLR translations and loading translation models are generally better at the annual frequency, except for the annual signal amplitude of the Z component. However, the high frequencies of such model translations do not explain SLR translation short-term variability. We reach similar conclusions with both approaches which proves the existence of this effect. SLR products and the two loading models studied here are consequently accurate enough to be used together to detect the network effect.

[68] In the most recent ITRF computation, apparent geocenter motion was estimated simultaneously with secular reference frames for each contributing technique solution [*Altamimi et al.*, 2007] by means of translations estimates. Time series of net scale (radial) changes were obtained in that processing as well. Analysis of the translation and scale parameters is useful to assess technique systematic errors and to evaluate which observations should be used to fix the ITRF datum specifications. We attempted to clarify the nature of observed SLR translation and scale variability in this study. Estimating Helmert parameters when processing a secular terrestrial reference frame is not the only approach used in reference frame analysis. Another approach is, for example, presented by *Davies and Blewitt* [2000]. Our study conducted using quite independent loading models only explained most of the annual variations in translations and scale, which indicates that other types of variations are related to noise or modeling errors. As a consequence, this work shows that estimating translation and scale parameters when stacking SLR frame data is relevant. Of course, the study of the scale itself is not the optimal way to understand SLR systematic errors since its variation could result from aliasing due to a variety of station height errors. However, the scale parameter is relevant in reference frame analysis and estimating it is a quick way to evaluate the time series of reference frames. Since not all the SLR scale scatter is understood, although range biases could be responsible for part of it [*Coulot et al.*, 2008], we still advise estimating this parameter. Moreover, we have shown here that neglecting the scale parameter is not sufficient to limit the network effect on the X translation component especially. As this study indicates that the annual signal in the SLR scale is mostly due to the SLR station ground motion, it could be worth correcting weekly SLR frames with a loading model before stacking them to estimate secular terrestrial reference frames. Such studies should be investigated in the near future and the impact on the ITRF itself should be investigated further.

[69] This study secondarily aimed to study the agreement between SLR data and geocenter motion models. The level of agreement between the two considered models and the SLR data is not yet perfect but quite satisfying. The annual signals and Z component semiannual signals are notably quite well recovered by SLR, the forward loading model and the loading mass coefficients inversion method. The agreement at other periods is promising: it seems that significant interannual variation is present in both ILRS data and the inverse model for the X component. However, those are not seen in the forward model. This rather good agreement and other recent work on inverse modeling [*Lavallée et al.*, 2006] are very encouraging. It seems that a common signal is clearly seen in all the data sources. This could prompt the IERS to reconsider a conventional geocenter motion model, at least at the seasonal timescale. This issue was addressed earlier [*Ray*, 1999; *Dong et al.*, 2003] but agreement among observational results has greatly improved since that time. Such a model could be either a single or a multitechnique combination if it is demonstrated that each model can contribute some strength. We have a good illustration with this study that SLR and GPS are complementary techniques.

Appendix A

[70] As the GPS/OBP loading model has a known covariance matrix (singular due to the model spatial resolution), it could be used to re-evaluate the Helmert parameters variance as follows

$$\Sigma = \left(A^T P A\right)^{-1} A^T P \Sigma_{dX} P A \left(A^T P A\right)^{-1} \quad , \tag{A1}$$

with P the weight matrix being used in the estimation of the transformation parameters, namely $P = \Sigma_{SLR}^{-1}$ and Σ_{dX} the covariance matrix of the loading model and

$$A = \begin{pmatrix} \vdots & \vdots & \vdots & \vdots & \vdots & \vdots & \vdots \\ 1 & 0 & 0 & x_0 & 0 & z_0 & -y_0 \\ 0 & 1 & 0 & y_0 & -z_0 & 0 & x_0 \\ 0 & 0 & 1 & z_0 & y_0 & -x_0 & 0 \\ \vdots & \vdots & \vdots & \vdots & \vdots & \vdots & \vdots \end{pmatrix}, \tag{A2}$$

where (x_0, y_0, z_0) are approximate coordinates of the corresponding point.

Appendix B

[71] We define the percentage of WRMS reduction for the parameter p following *van Dam et al.* [2007] as

$$100 \cdot \frac{WRMS[p_1] - WRMS[p_1 - p_2]}{WRMS[p_1]}, \tag{B1}$$

where p_1 and p_2 are two estimations of the parameter p. In the application to translation and scale, we have computed the WRMS with respect to zero mean.

[72] **Acknowledgments.** We are grateful to Hans-Georg Scherneck, David Coulot, and Laurent Métivier for useful discussions. We wish to thank David Lavallée, the associate editor Pedro Elosegui, and an anonymous reviewer for their constructive comments. X. Wu thanks Danan Dong and Susan Owen for their efforts in computing the GPS time series used in the inverse model. Part of this research was carried out at the Jet Propulsion Laboratory, California Institute of Technology, under a contract with the National Aeronautics and Space Administration. The bottom pressure estimates were provided by the ECCO Consortium for Estimating the Circulation and Climate of the Ocean funded by the National Oceanographic Partnership Program (NOPP). All the plots have been made with the General Mapping Tool (GMT) software [*Wessel and Smith*, 1991], available at http://gmt.soest.hawaii.edu/ under the GNU General Public License.

References

Altamimi, Z., P. Sillard, and C. Boucher (2002), ITRF2000: A new release of the International Terrestrial Reference Frame for earth science applications, *J. Geophys. Res.*, *107*(B10), 2214, doi:10.1029/2001JB000561.

Altamimi, Z., P. Sillard, and C. Boucher (2003), ITRF2000: From theory to implementation, in *V Hotine-Marussi Symposium on Mathematical Geodesy, IAG Symposia*, vol. 127, edited by F. Sansò, pp. 157–163, Springer, New York.

Altamimi, Z., X. Collilieux, J. Legrand, B. Garayt, and C. Boucher (2007), ITRF2005: A new release of the International Terrestrial Reference Frame based on time series of station positions and Earth Orientation Parameters, *J. Geophys. Res.*, *112*, B09401, doi:10.1029/2007JB004949.

Altamimi, Z., X. Collilieux, and C. Boucher (2008), Accuracy Assessment of the ITRF Datum Definition, in *Proceedings of VI Hotine-Marussi Symposium of Theoretical and Computational Geodesy, IAG Symposia*, vol. 132, edited by P. Xu, J. Liu, and A. Dermanis, pp. 101–110, Springer, New York.

Blewitt, G. (2003), Self-consistency in reference frames, geocenter definition, and surface loading of the solid Earth, *J. Geophys. Res.*, *108*(B2), 2103, doi:10.1029/2002JB002082.

Blewitt, G., Y. Bock, and J. Kouba (1994), Constraining the IGS polyhedron by distributed processing, in *Densification of ITRF Through Regional GPS Networks*, 2137 pp., IGS Cent. Bur., Jet Propul. Lab., Pasadena, Calif.

Blewitt, G., D. Lavallée, P. Clarke, and K. Nurutdinov (2001), A new global mode of Earth deformation: Seasonal cycle detected, *Science*, *294*, 2342–2345.

Bouillé, F., A. Cazenave, J. M. Lemoine, and J. F. Crétaux (2000), Geocentre motion from the DORIS space system and laser data to the Lageos satellites: Comparison with surface loading data, *Geophys. J. Int.*, *143*, 71–82, doi:10.1046/j.1365-246x.2000.00196.x.

Chen, J. L., C. R. Wilson, R. J. Eanes, and R. S. Nerem (1999), Geophysical interpretation of observed geocenter variations, *J. Geophys. Res.*, *104*(B2), 2683–2690.

Cheng, M. (1999), Geocenter variations from analysis of Topex/Poseidon SLR data, in *IERS Tech. Note 25*, edited by J. Ray, pp. 39–40, IERS, Observatoire de Paris, Paris.

Clarke, P. J., D. A. Lavallée, G. Blewitt, T. M. van Dam, and J. M. Wahr (2005), Effect of gravitational consistency and mass conservation on seasonal surface mass loading models, *Geophys. Res. Lett.*, *32*, L08306, doi:10.1029/2005GL022441.

Clarke, P. J., D. A. Lavallée, G. Blewitt, and T. van Dam (2007), Basis functions for the consistent and accurate representation of surface mass loading, *Geophys. J. Int.*, *171*, 1–10, doi:10.1111/j.1365-246X.2007.03493.x.

Collilieux, X., Z. Altamimi, D. Coulot, J. Ray, and P. Sillard (2007), Comparison of very long baseline interferometry, GPS, and satellite laser ranging height residuals from ITRF2005 using spectral and correlation methods, *J. Geophys. Res.*, *112*, B12403, doi:10.1029/2007JB004933.

Coulot, D., P. Berio, P. Bonnefond, P. Exertier, D. Féraudy, O. Laurain, and F. Deleflie (2008), Satellite Laser Ranging biases and Terrestrial Reference Frame scale factor, in *Observing Our Changing Planet, International Association of Geodesy Symposia*, vol. 133, pp. 39–46, Springer, New York, doi:10.1007/978-3-540-85426-5.

Crétaux, J.-F., L. Soudarin, F. J. M. Davidson, M.-C. Gennero, M. Bergé-Nguyen, and A. Cazenave (2002), Seasonal and interannual geocenter motion from SLR and DORIS measurements: Comparison with surface loading data, *J. Geophys. Res.*, *107*(B12), 2374, doi:10.1029/2002JB001820.

Davies, P., and G. Blewitt (2000), Methodology for global geodetic time series estimation: A new tool for geodynamics, *J. Geophys. Res.*, *105*(B5), 11,083–11,100.

Davis, J. L., P. Elósegui, J. X. Mitrovica, and M. E. Tamisiea (2004), Climate-driven deformation of the solid Earth from GRACE and GPS, *Geophys. Res. Lett.*, *31*, L24605, doi:10.1029/2004GL021435.

Devoti, R., M. Fermi, C. Sciarretta, V. Luceri, R. Pacione, F. Rutigliano, and P. Vespe (1999), CGS geocenter time series from SLR and GPS data, in *IERS Tech. Note 25*, edited by J. Ray, pp. 41–46, IERS, Observatoire de Paris, Paris.

Dong, D., J. O. Dickey, Y. Chao, and M. K. Cheng (1997), Geocenter variations caused by atmosphere, ocean and surface ground water, *Geophys. Res. Lett.*, *24*(15), 1867–1870.

Dong, D., P. Fang, Y. Bock, M. K. Cheng, and S. Miyazaki (2002), Anatomy of apparent seasonal variations from GPS-derived site position time series, *J. Geophys. Res.*, *107*(B4), 2075, doi:10.1029/2001JB000573.

Dong, D., T. Yunck, and M. Heflin (2003), Origin of the International Terrestrial Reference Frame, *J. Geophys. Res.*, *108*(B4), 2200, doi:10.1029/2002JB002035.

Eanes, R. J., S. Kar, S. V. Bettadpur, and M. M. Watkins (1997), Low-frequency geocenter motion determined from SLR tracking (abstract), *Eos Trans. AGU*, *78*(46), Fall Meet. Suppl., F146.

Farrell, W. E. (1972), Deformation of the Earth by surface loads, *Rev. Geophys.*, *10*(3), 761–797.

Feissel-Vernier, M., K. Le Bail, P. Berio, D. Coulot, G. Ramillien, and J.-J. Valette (2006), Geocentre motion measured with DORIS and SLR, and predicted by geophysical models, *J. Geod.*, *80*(8–11), 637–648, doi:10.1007/s00190-006-0079-z.

Greff-Lefftz, M., and H. Legros (1997), Some remarks about the degree-one deformation of the Earth, *Geophys. J. Int.*, *131*, 699–723, doi:10.1111/j.1365-246X.1997.tb06607.x.

Hugentobler, U., S. Schaer, D. R. M. Meindl, C. Urshl, and G. Beutler (2005), Relevance of GNSS geocenter for precise point positioning, paper presented at the European Geosciences Union General Assembly, Vienna, 24–29 Apr.

Jet Propulsion Laboratory (JPL) (2008), Ecco ocean data assimilation, http://ecco.jpl.nasa.gov/.

Kouba, J., J. Ray, and M. Watkins (1998), IGS Reference Frame Realization, in *IGS Workshop Proceedings: 1998 Analysis Center Workshop*, edited by T. S. J. M. Dow and J. Kouba, pp. 139–171, European Space Operations Centre, Darmstadt, Germany.

Kusche, J., and E. J. O. Schrama (2005), Surface mass redistribution inversion from global GPS deformation and Gravity Recovery and Climate Experiment (GRACE) gravity data, *J. Geophys. Res.*, *110*, B09409, doi:10.1029/2004JB003556.

Lavallée, D. A., T. van Dam, G. Blewitt, and P. J. Clarke (2006), Geocenter motions from GPS: A unified observation model, *J. Geophys. Res.*, *111*, B05405, doi:10.1029/2005JB003784.

Luceri, V., and E. Pavlis (2006), The ILRS solution, technical report, ILRS Tech. Rep. (Available at http://itrf.ensg.ign.fr/ITRF_solutions/2005/doc/ILRS_ITRF2005_description.pdf)

McCarthy, D. D., and G. Petit (Eds.) (2004), *IERS Conventions (2003)*, *IERS Tech. Note 32*, Verlag des Bundesamts für Kartographie und Geodäsie, Frankfurt am Main.

Milly, P. C. D., and A. B. Shmakin (2002), Global modeling of land water and energy balances. part I: The land dynamics (LaD) model, *J. Hydrometeorol.*, *3*, 283–299.

Moore, P., and J. Wang (2003), Geocentre variation from laser tracking of LAGEOS1/2 and loading data, *Adv. Space Res.*, *31*, 1927–1933, doi:10.1016/S0273-1177(03)00170-4.

NOAA (1988), Digital relief of the surface of the earth, NOAA, Natl. Geophys. Data Cent., Boulder, Colo.

Pavlis, H. (1999), Fortnightly Resolution geocenter series: A combined analysis of Lageos 1 and 2 SLR data (1993–96), in *IERS Tech. Note 25*, edited by J. Ray, pp. 75–84, IERS, Observatoire de Paris, Paris.

Ray, J. (Ed.) (1999), *IERS Analysis Campaign to Investigate Motions of the Geocenter*, *IERS Tech. Note 25*, Observatoire de Paris, Paris.

Shmakin, A. B., P. C. D. Milly, and K. A. Dunne (2002), Global modeling of land water and energy balances. part III: Interannual variability, *J. Hydrometeorol.*, *3*, 311–321.

Springer, T. (2000), IGS Final orbit changes, *IGS Mail 2750*. (Available at http://igscb.jpl.nasa.gov/mail/igsmail/2000/msg00090.html)

Swenson, S., D. Chambers, and J. Wahr (2008), Estimating geocenter variations from a combination of GRACE and ocean model output, *J. Geophys. Res.*, *113*, B08410, doi:10.1029/2007JB005338.

Trupin, A. S., M. F. Meier, and J. M. Wahr (1992), Effect of melting glaciers on the Earth's rotation and gravitational field: 1965–1984, *Geophys. J. Int.*, *108*, 1–15, doi:10.1111/j.1365-246X.1992.tb00835.x.

van Dam, T. M., and J. M. Wahr (1987), Displacements of the earth's surface due to atmospheric loading: Effects of gravity and baseline measurements, *J. Geophys. Res.*, *92*(B2), 1281–1286.

van Dam, T., J. Wahr, and D. Lavallée (2007), A comparison of annual vertical crustal displacements from GPS and Gravity Recovery and Climate Experiment (GRACE) over Europe, *J. Geophys. Res.*, *112*, B03404, doi:10.1029/2006JB004335.

Watkins, M. M., and R. J. Eanes (1997), Observations of tidally coherent diurnal and semidiurnal variations in the geocenter, *Geophys. Res. Lett.*, *24*(17), 2231–2234.

Wessel, P., and W. H. F. Smith (1991), Free software helps map and display data, *Eos Trans. AGU*, *72*, 441, doi:10.1029/90EO00319.

Wu, X., D. F. Argus, M. B. Heflin, E. R. Ivins, and F. H. Webb (2002), Site distribution and aliasing effects in the inversion for load coefficients and geocenter motion from GPS data, *Geophys. Res. Lett.*, *29*(24), 2210, doi:10.1029/2002GL016324.

Wu, X., M. B. Heflin, E. R. Ivins, D. F. Argus, and F. H. Webb (2003), Large-scale global surface mass variations inferred from GPS measurements of load-induced deformation, *Geophys. Res. Lett.*, *30*(14), 1742, doi:10.1029/2003GL017546.

Wu, X., M. B. Heflin, E. R. Ivins, and I. Fukumori (2006), Seasonal and interannual global surface mass variations from multisatellite geodetic data, *J. Geophys. Res.*, *111*, B09401, doi:10.1029/2005JB004100.

Z. Altamimi and X. Collilieux, Laboratoire de Recherche en Géodésie, Institut Géographique National, 6-8 Avenue Blaise Pascal, Cité Descartes - Champs-sur-Marne, F-77455 Marne-La-Vallée Cedex 2, France. (xavier.collilieux@ign.fr)

J. Ray, NOAA National Geodetic Survey, 1315 East-West Highway, Silver Spring, MD 20910, USA. (jimr@ngs.noaa.gov)

T. van Dam, Department of Physics and Material Sciences, University of Luxembourg, 162a, avenue de la Faïencerie, L-1511 Luxembourg, Luxembourg. (tonie.vandam@uni.lu)

X. Wu, Jet Propulsion Laboratory, California Institute of Technology, 4800 Oak Grove Drive, Pasadena, CA 91109-8099, USA. (Xiaoping.Wu@jpl.nasa.gov)